Supplementary Information (SI) for Journal of Materials Chemistry C.

Immobilization of laccase on functional groups and degree of conjugation modified COFs for simultaneous Photochemical-Enzymatic removal of 2,4-dichlorophenol and uranium U(VI)

Xin Zhong*, Zhehong Ji, Qian Ling, Lifu Sun, Baowei Hu

School of Life and Environmental Sciences, Shaoxing University, Huancheng West Road 508, Shaoxing 312000, P.R. China

Corresponding author e-mail:

Xin Zhong: zhongxinmagic@163.com

1. Chemicals

1,3,5-triformylphloroglucinol (Tp, 97%) was obtained from Jilin Yanshen Technology (China). Laccase (from *Trametes versicolor*, 0.5 U·mg^{-1}, EC 1.10.3.2), 2,4-dichlorophenol (2,4-DCP), glutaraldehyde (GA, 25 % in v/v, aqueous solution), $UO_2(NO_3)_2·6H_2O$ (99.5%), mesitylene (98%), acetic acid (99.5%), 1,4-dioxane (99.5%), 2,2′-azino-bis(3-ethylbenzothiazoline-6-sulfonic acid (ABTS, 99%), 1,4-diaminobenzene (Pa-1, 99%), benzidine (BD, 97%), 4,4"-Diamino-p-terphenyl (TPA, 98%), 2,5-diaminohydroquinone dihydrochloride (Pa-$(OH)_2$·2HCl, 97%), 2-nitro-1,4-phenelynediamine (Pa-NO_2, 98%), 3,3′-dinitrobenzidine (BD(-NO_2)$_2$, 95%), 3,3′-dihydroxybenzidine (BD(-OH)$_2$, 99%) and other reagents were purchased from Macklin Biochemistry Co., Ltd (Shanghai, China).

2. Characterization

XRD spectra were obtained on a Bruker D8 diffractometer. FT-IR spectra were collected on a ThermoFisher Nicolet NEXUS 670 spectrophotometer. The morphologies of COFs-TpPa-X were photographed on SEM (JEOL-7800F) and HRTEM-Mapping (HAADF-STEM, JEOL-2100F). Thermogravimetric analysis (TGA) was conducted on a SDT650-TA Instruments by heating from 20 to 800 °C with 10 °C/min in N_2 atmosphere. The BET specific surface areas were obtained from Micromeritics ASAP 2020 apparatus. XPS analysis and work function calculation (PS spectra, He lamp 21.21 eV) were performed measured on using a Thermo Fisher ESCALAB 250Xi. The UV-visible diffused reflectance spectra (UV-vis DRS) were tested on a Shimadzu UV-2600 spectrophotometer with $BaSO_4$ as the background.

Confocal microscope images were captured by laser confocal scanning microscope (OLYMPUS FV1200). The electron spin resonance (ESR) spectra were detected by a Bruker MS 5000 instrument under visible light irradiation (300 W, lamp Au-Light). Free radicals $\bullet O_2^-$ and $^1O_2$ were detected by ESR using 5, 5-dimethyl-1-pyrroline-N-oxide (DMPO) and 2, 2, 6, 6tetramethyl-4-piperidinol (TEMP) as trapping agents, respectively. Transient photocurrent responses (*i*-*t*) and electrochemical impedance spectra (EIS) were carried out on a Shanghai Chenhua CHI 660E workstation with a standard three-electrode system.

3. Figures and tables

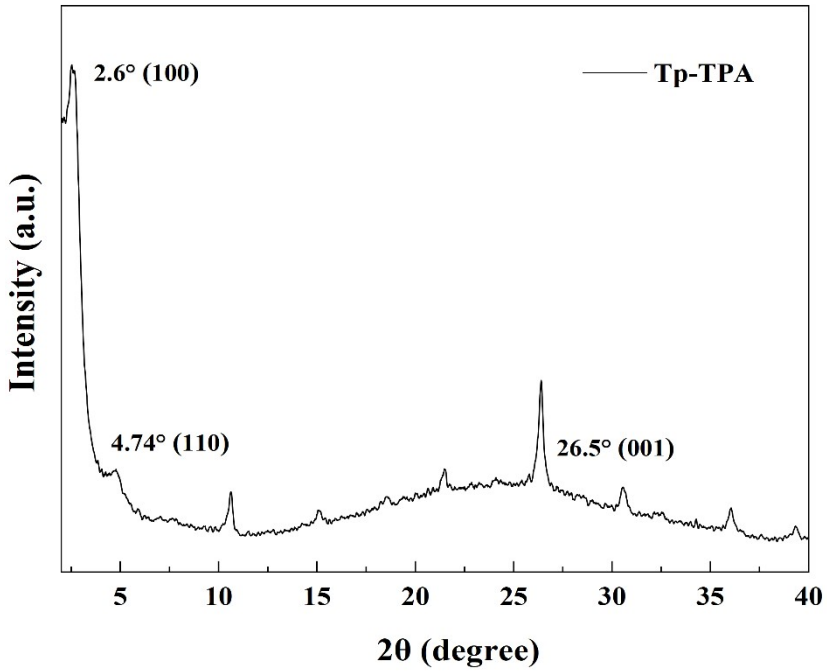

Fig. S1 The XRD pattern of Tp-TPA

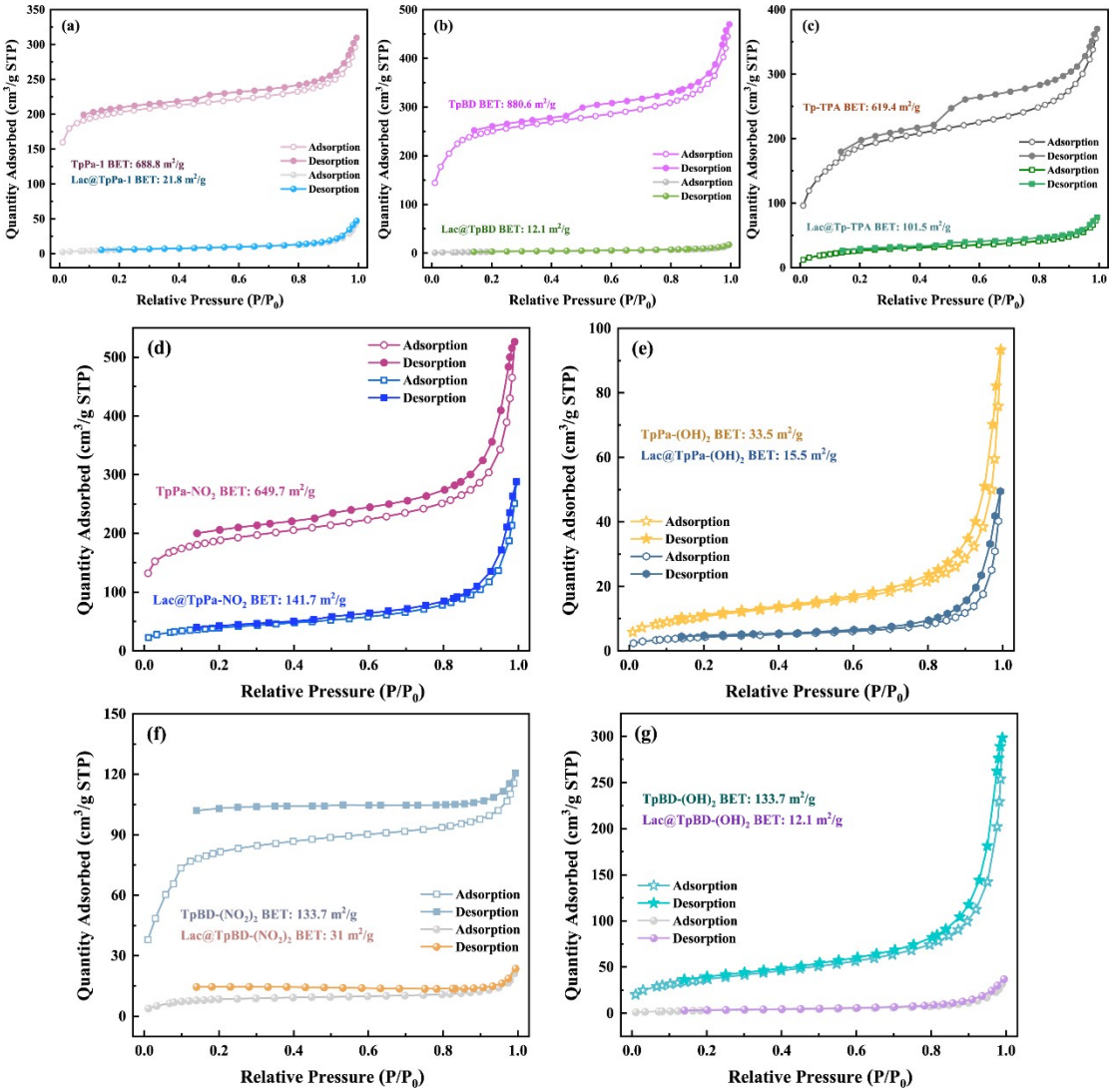

Fig. S2 The N_2 adsorption-desorption isotherms of COFs and laccase immobilized COFs.

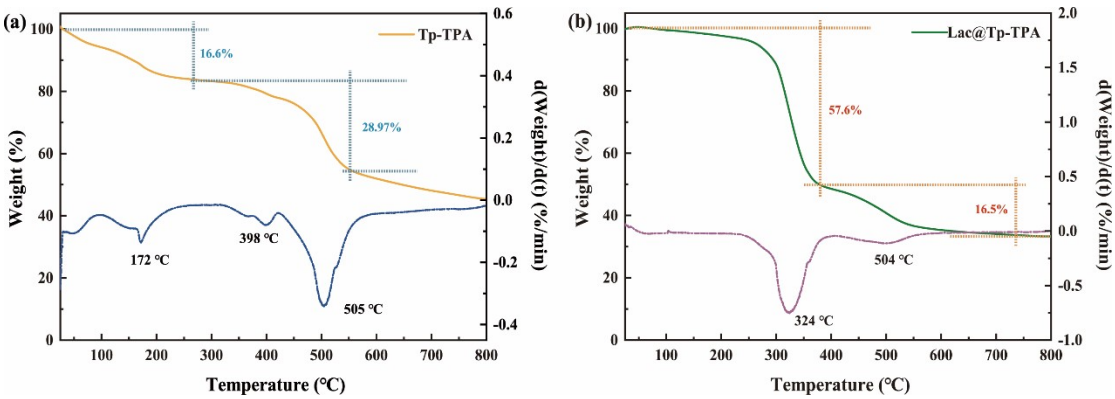

Fig. S3 The TGA curves of (a) Tp-TPA and (b) Lac@Tp-TPA.

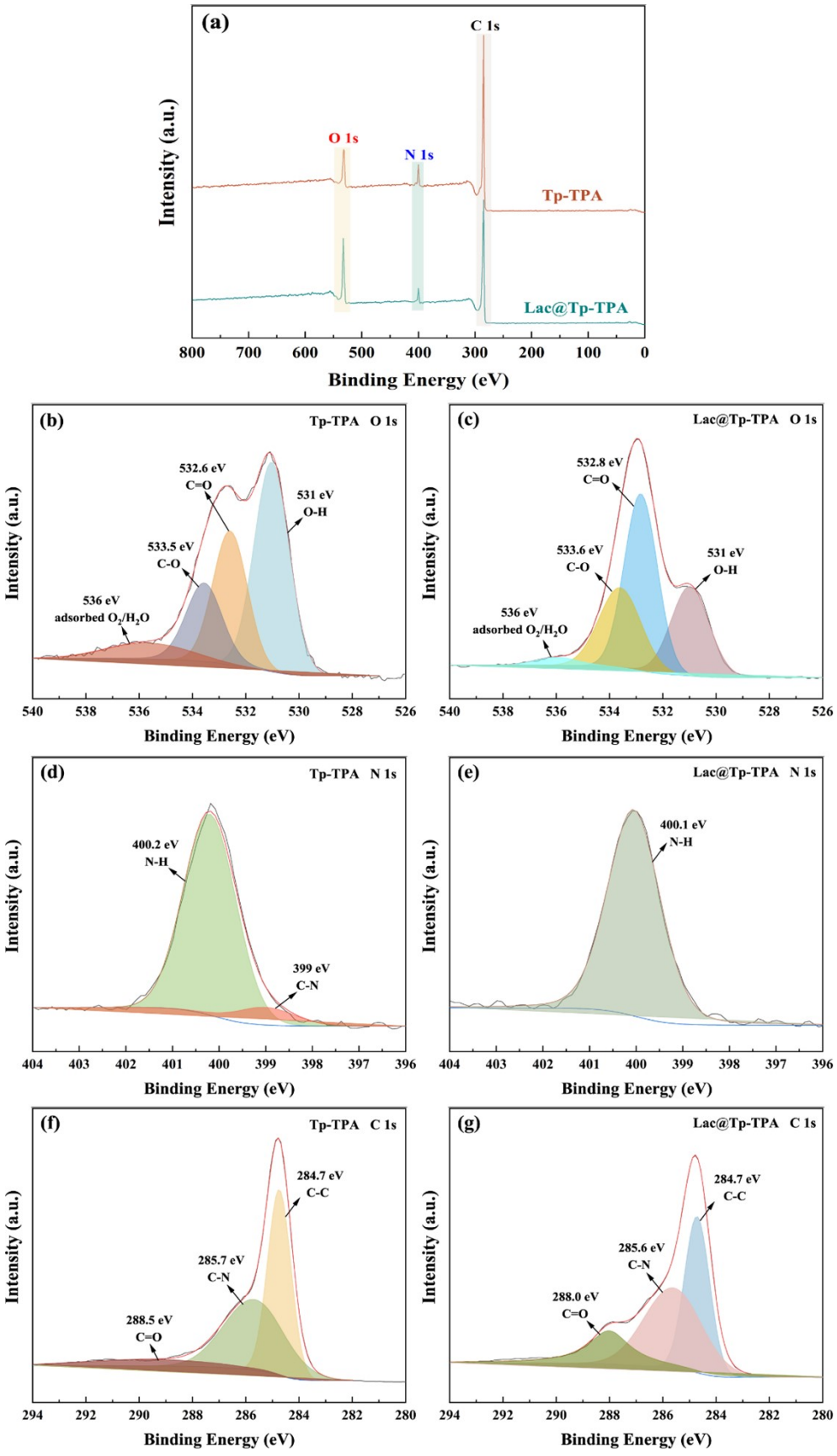

Fig. S4 (a) the XPS survey spectrum of Tp-TPA and Lac@Tp-TPA, the O 1s spectra of (b) Tp-TPA and (c) Lac@Tp-TPA, the N 1s spectra of (d) Tp-TPA and (e) Lac@Tp-TPA, the C 1s spectra of (f) Tp-TPA and (g) Lac@Tp-TPA.

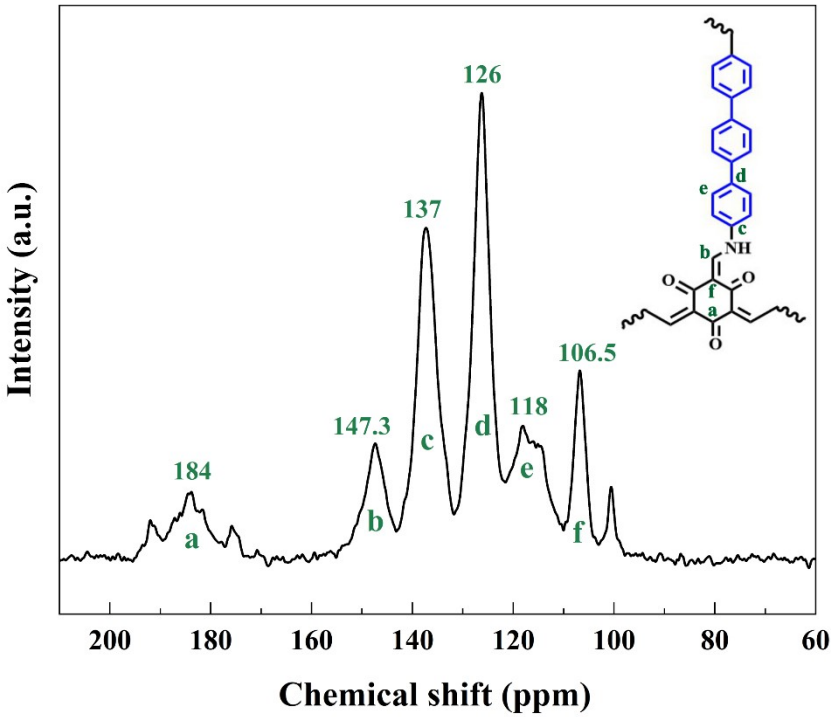

Fig. S5 Solid-state ^{13}C CP-MAS NMR spectrum of Tp-TPA.

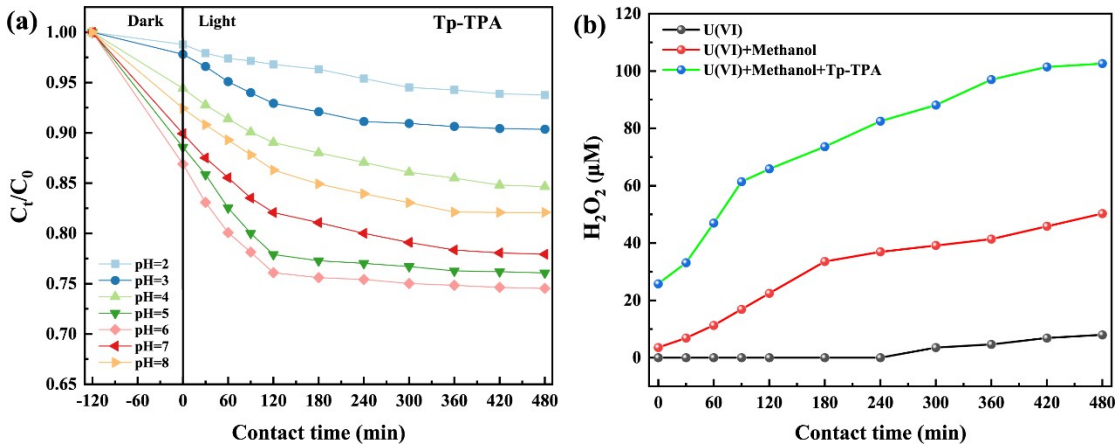

Fig. S6 (a) the performance of U(VI) photoreduction by Tp-TPA, (b) the generation of H_2O_2 during photo-immobilization of U(VI) in Tp-TPA system under visible light (C_0=30 mg/L, T=298 K, pH=5.0, m/V=0.1667 g/L, 3 mL CH_3OH).

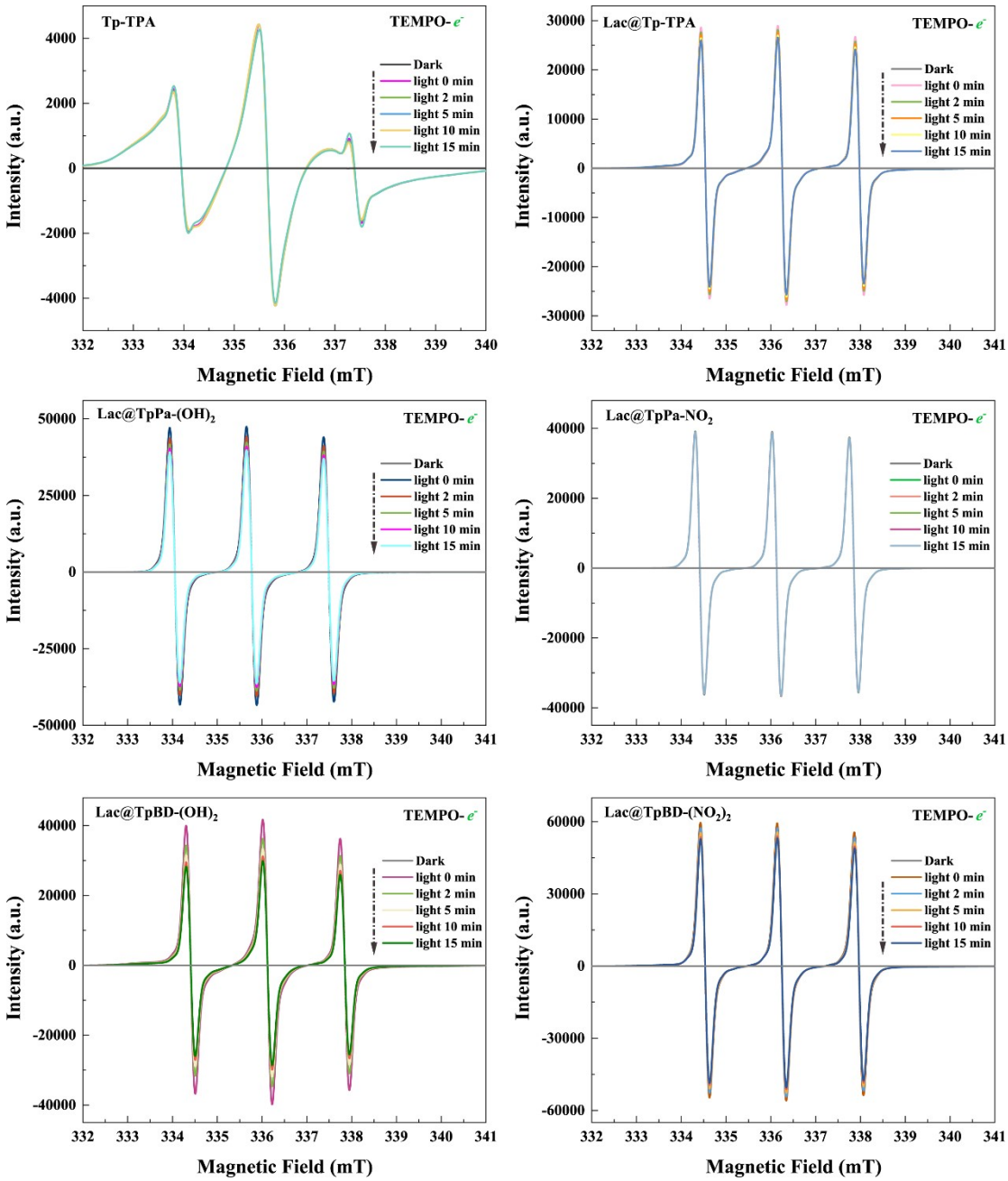

Fig. S7 The EPR spectra TEMPO-e^- of Tp-TPA and Lac@COFs under illumination for different times.

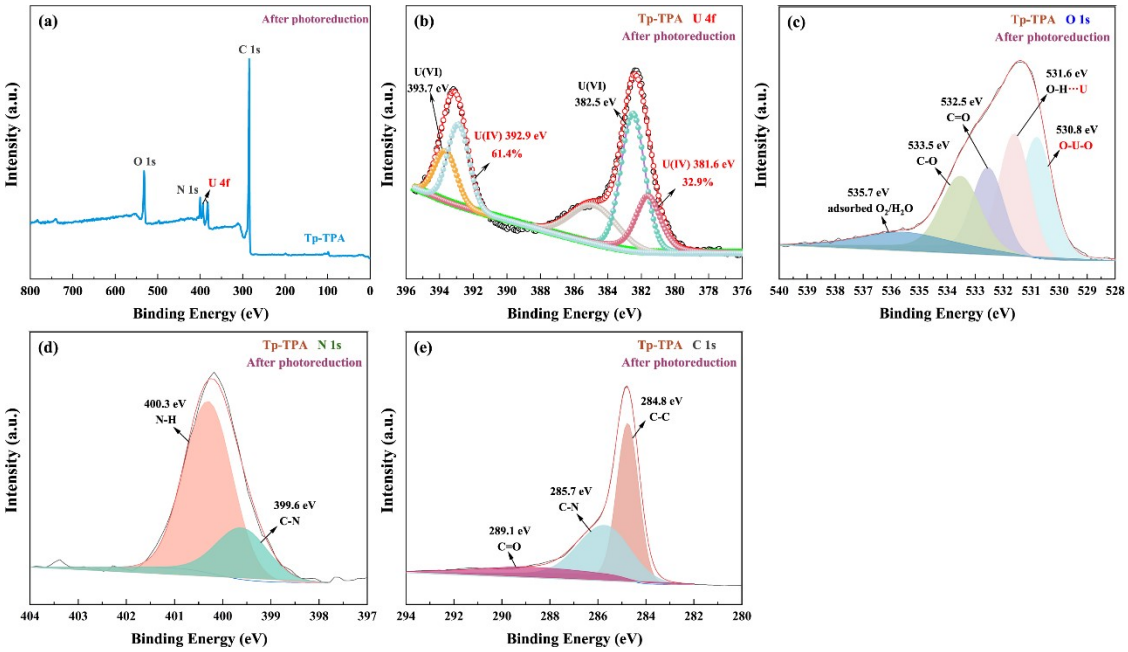

Fig. S8 (a) The XPS survey spectrum of Tp-TPA after photoreduction and the high-resolution (b) U 4f, (c) O 1s, (d) N 1s and (e) C 1s spectra of Tp-TPA after photoreduction.

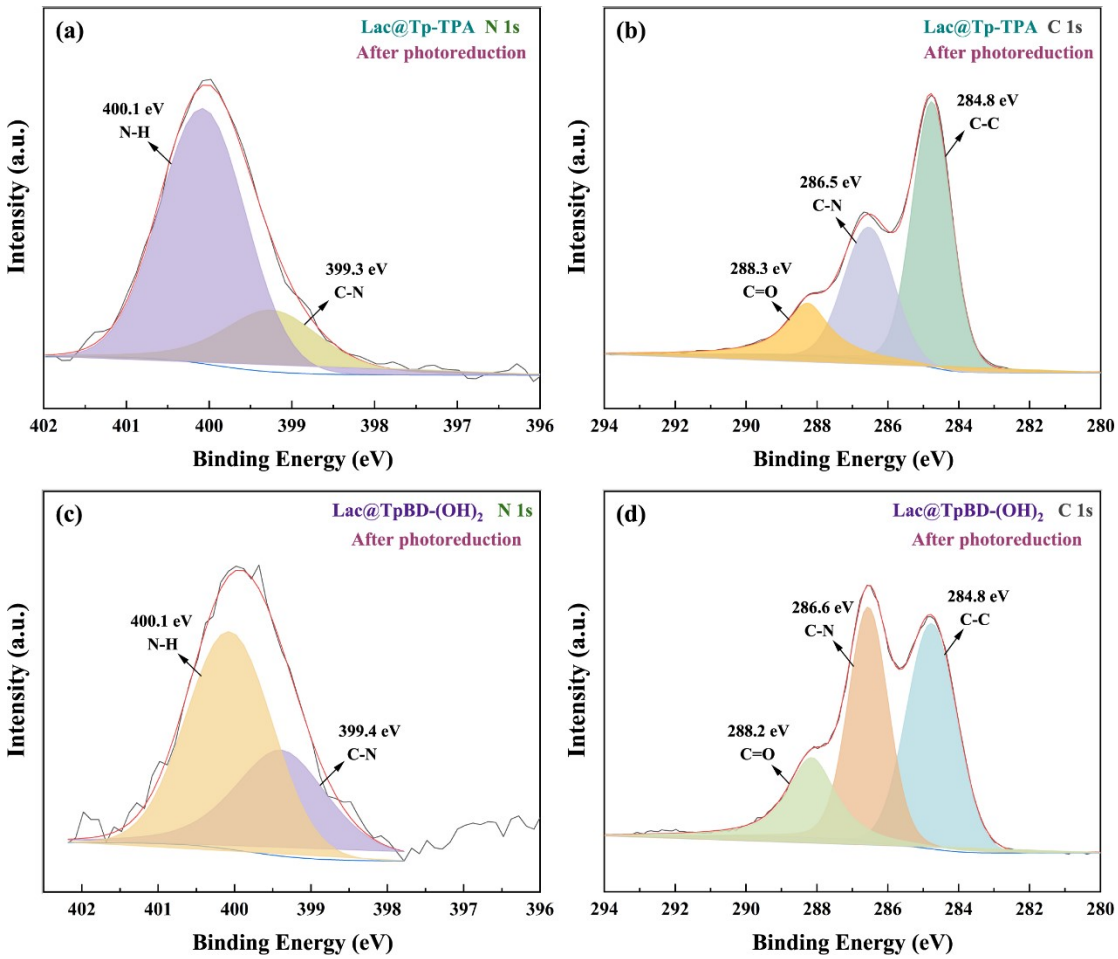

Fig. S9 The high-resolution (a) N 1s and (b) C 1s spectra of Lac@Tp-TPA after photoreduction, and the high-resolution (c) N 1s and (d) C 1s spectra of Lac@TpBD-$(OH)_2$ after photoreduction.

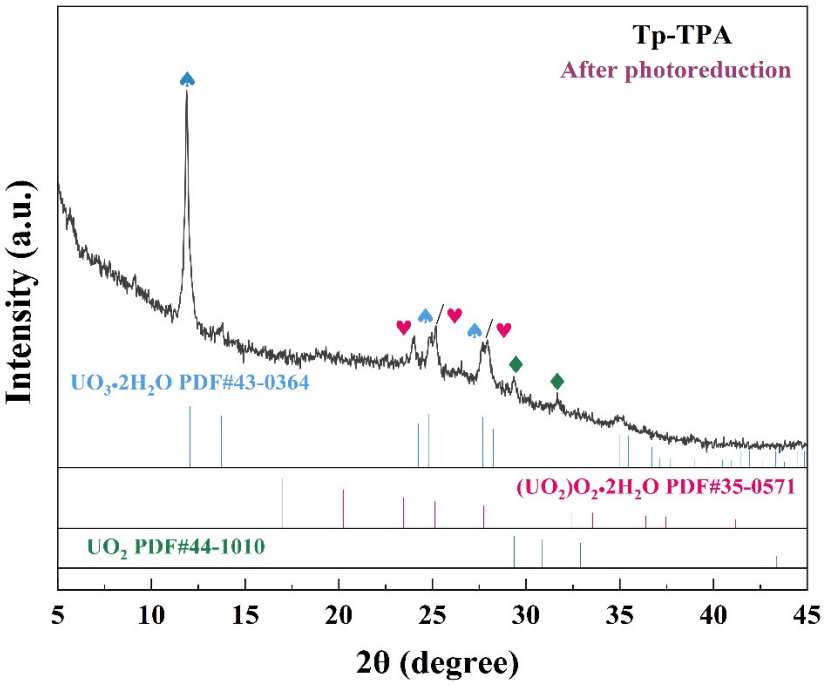

Fig. S10 The XRD pattern of Tp-TPA after U(VI) photoreduction under illumination.

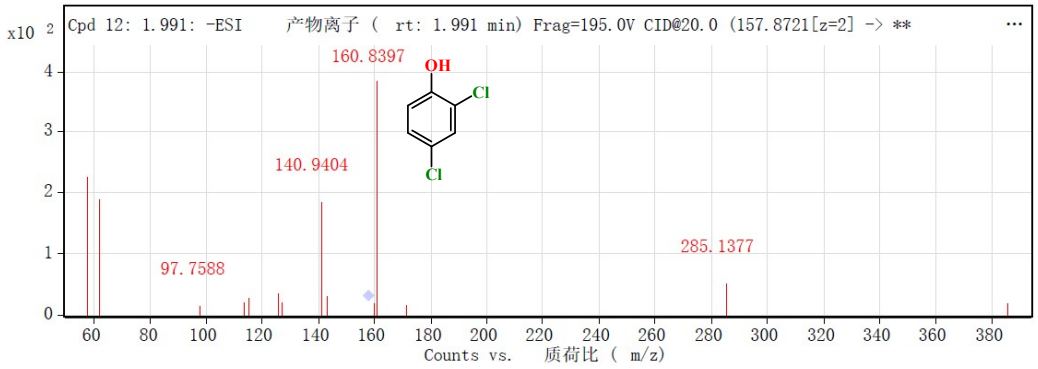

Fig. S11 The intermediates generated during 2,4-DCP degradation on Lac@Tp-TPA.

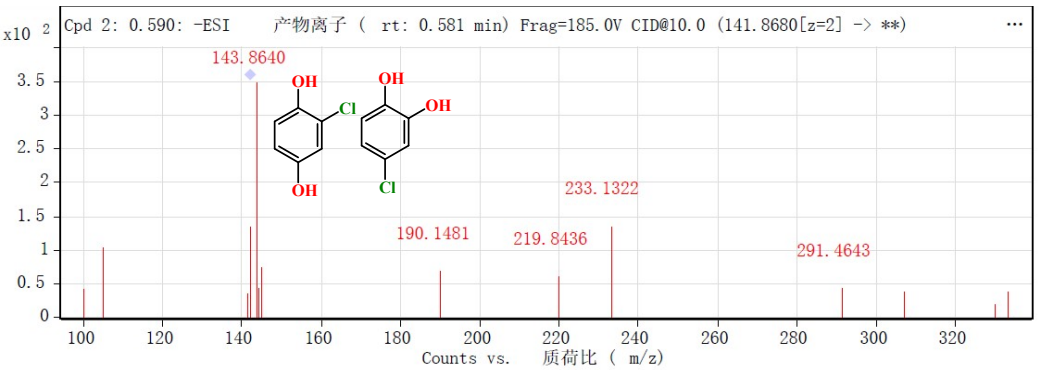

Fig. S12 The intermediates generated during 2,4-DCP degradation on Lac@Tp-TPA.

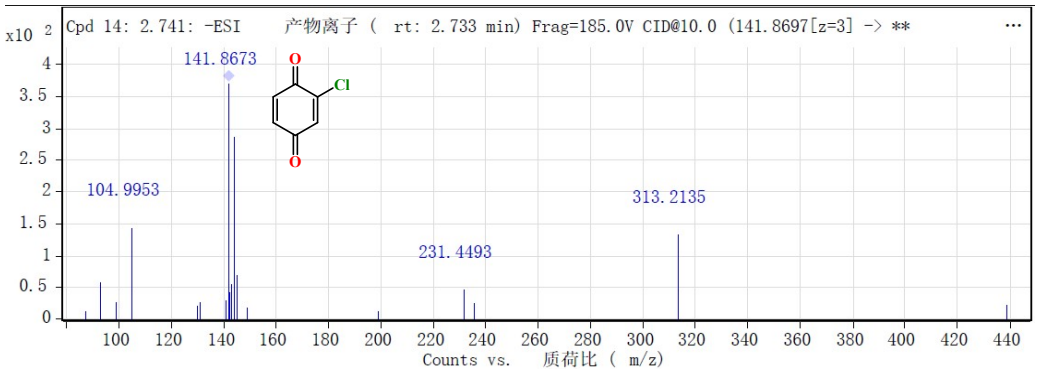

Fig. S13 The intermediates generated during 2,4-DCP degradation on Lac@Tp-TPA.

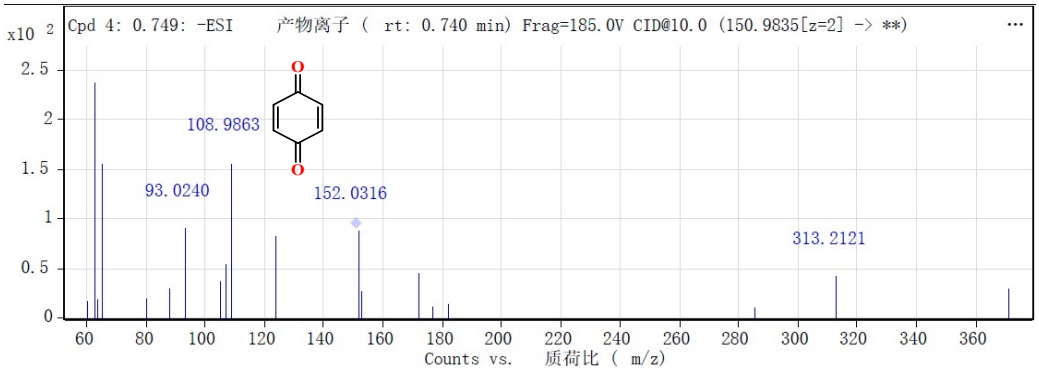

Fig. S14 The intermediates generated during 2,4-DCP degradation on Lac@Tp-TPA.

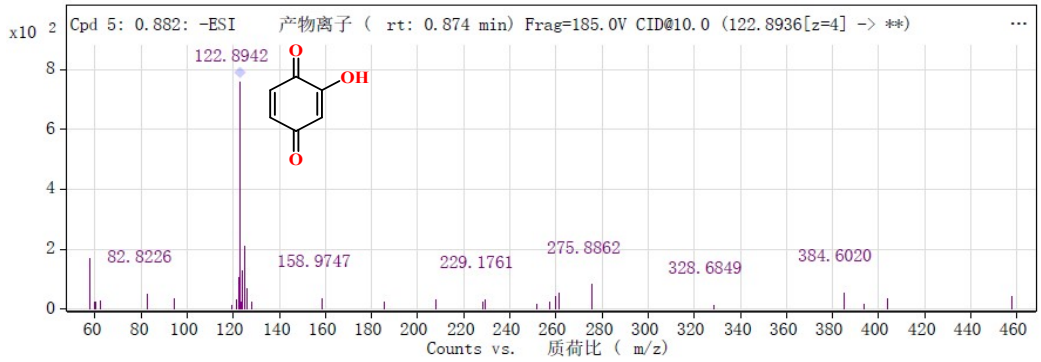

Fig. S15 The intermediates generated during 2,4-DCP degradation on Lac@Tp-TPA.

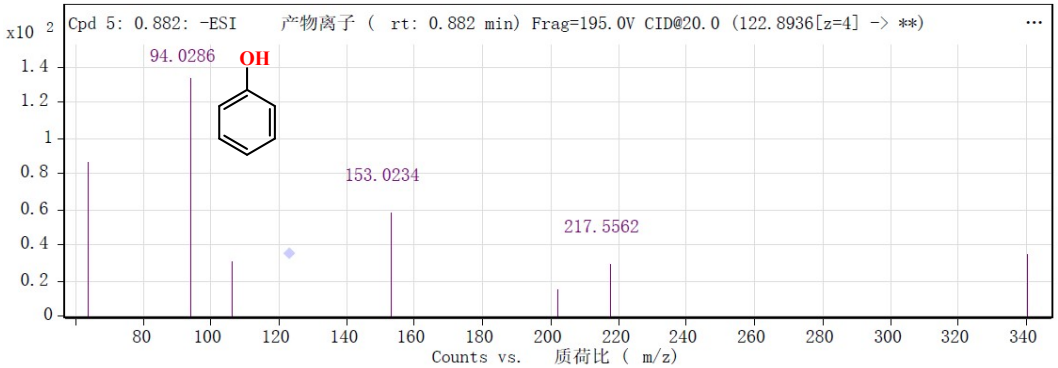

Fig. S16 The intermediates generated during 2,4-DCP degradation on Lac@Tp-TPA.

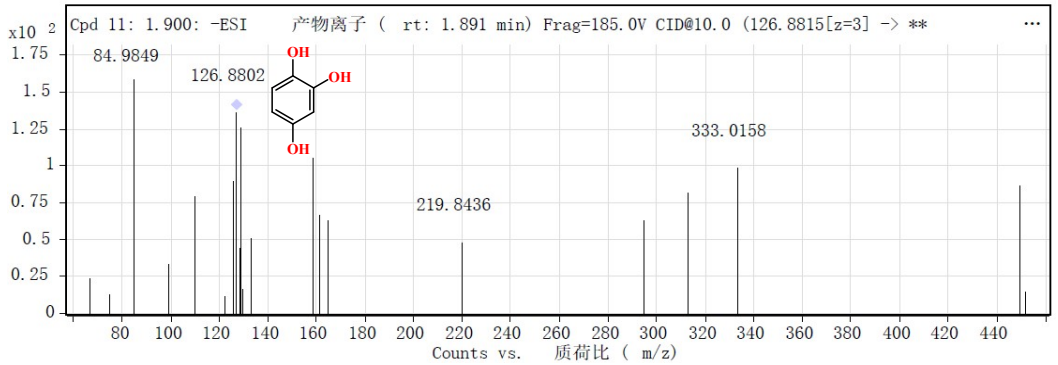

Fig. S17 The intermediates generated during 2,4-DCP degradation on Lac@Tp-TPA.

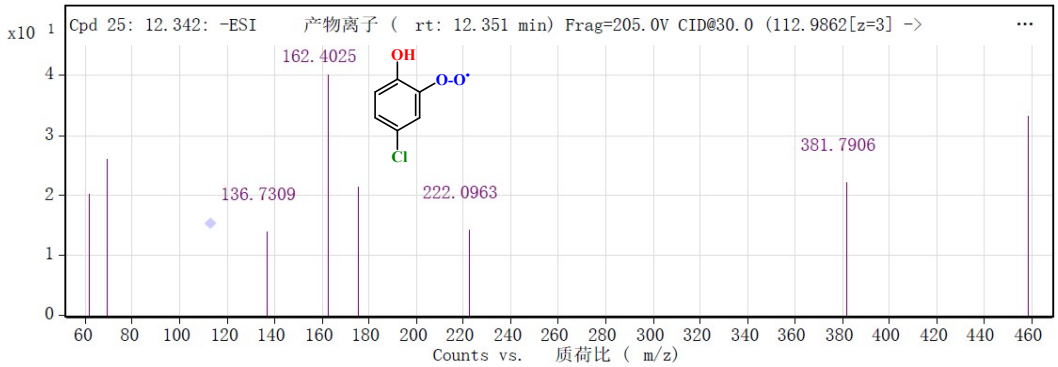

Fig. S18 The intermediates generated during 2,4-DCP degradation on Lac@Tp-TPA.

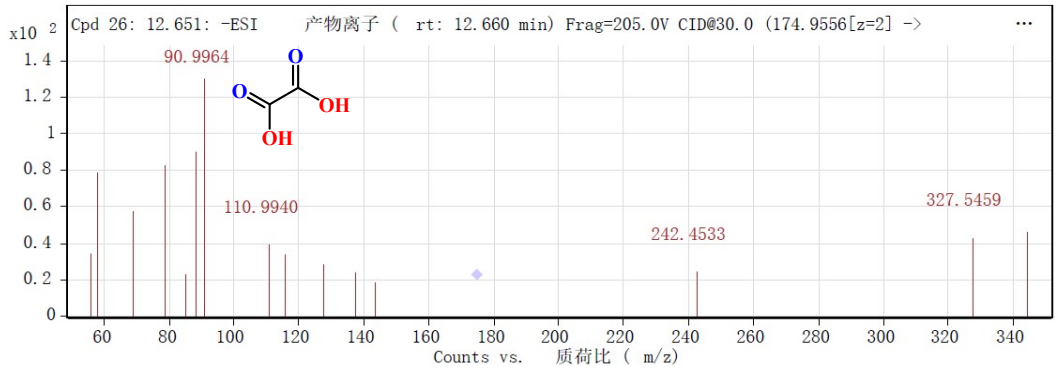

Fig. S19 The intermediates generated during 2,4-DCP degradation on Lac@Tp-TPA.

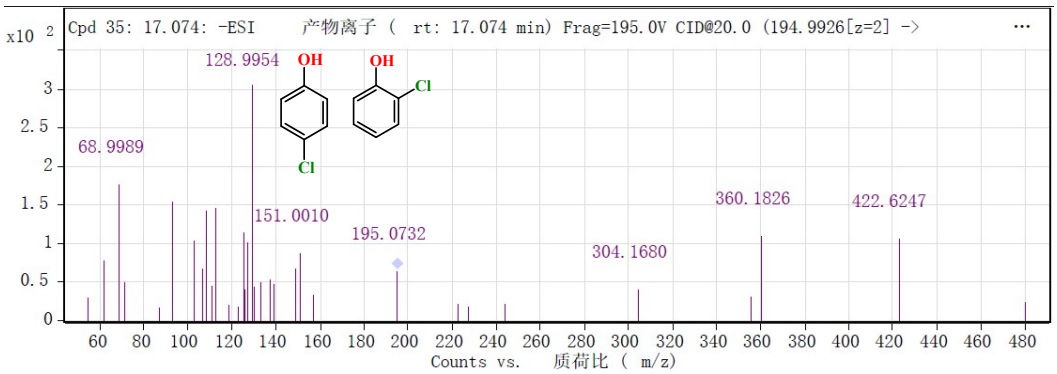

Fig. S20 The intermediates generated during 2,4-DCP degradation on Lac@Tp-TPA.

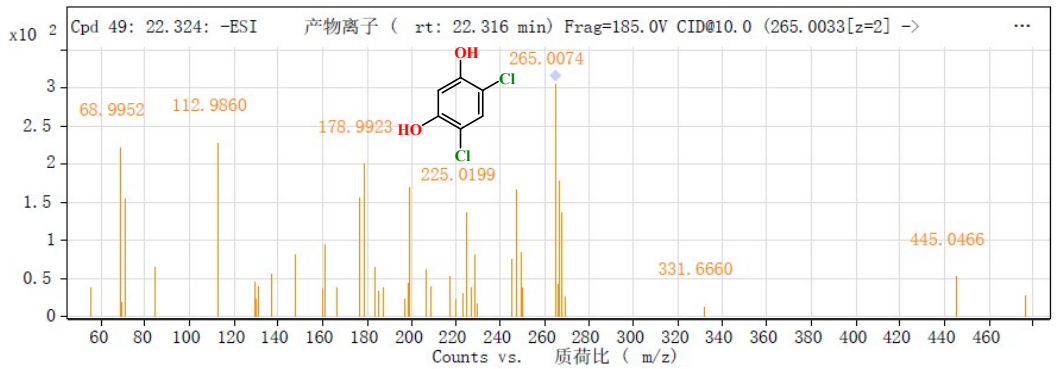

Fig. S21 The intermediates generated during 2,4-DCP degradation on Lac@Tp-TPA.

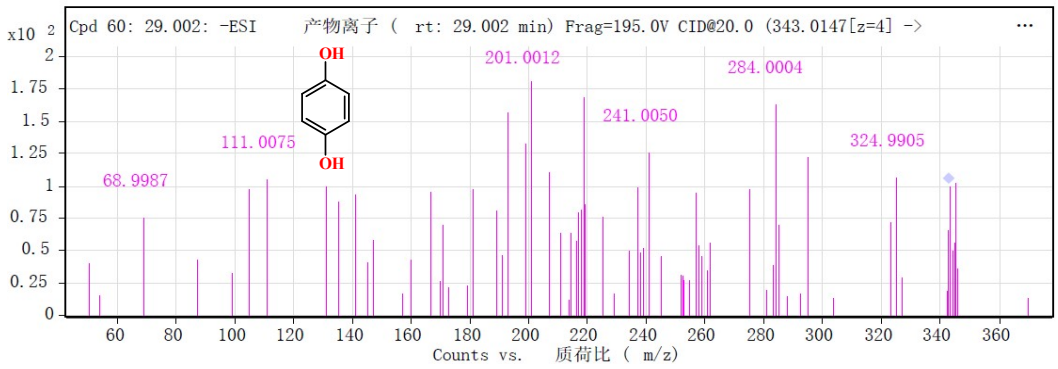

Fig. S22 The intermediates generated during 2,4-DCP degradation on Lac@Tp-TPA.

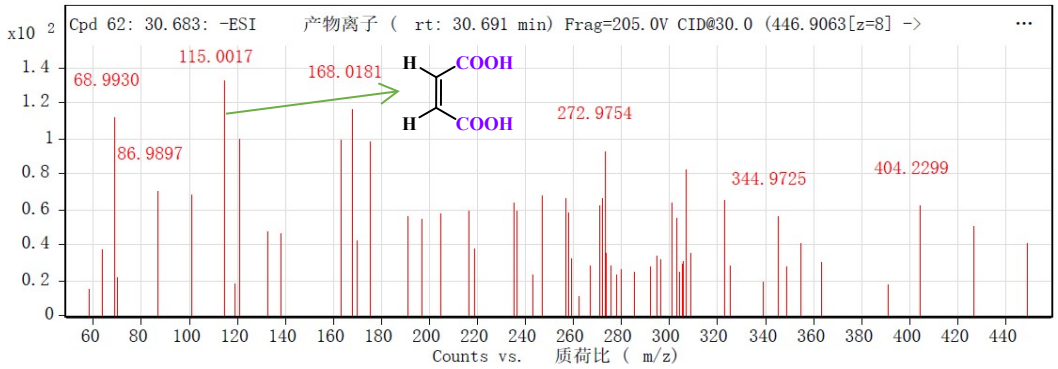

Fig. S23 The intermediates generated during 2,4-DCP degradation on Lac@Tp-TPA.

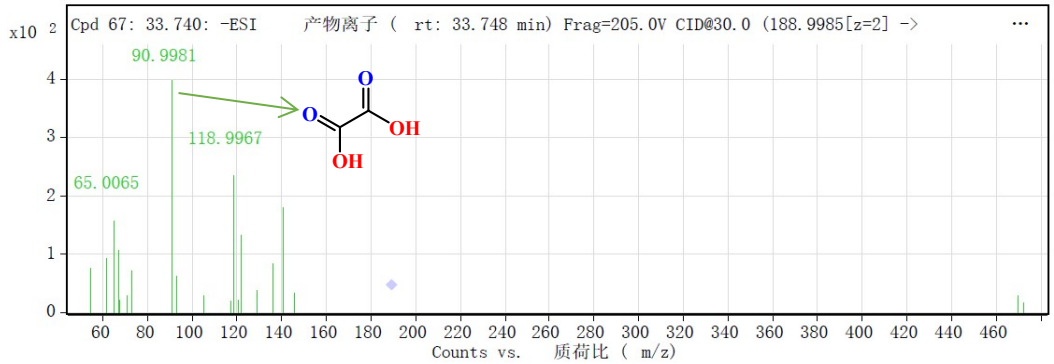

Fig. S24 The intermediates generated during 2,4-DCP degradation on Lac@Tp-TPA.

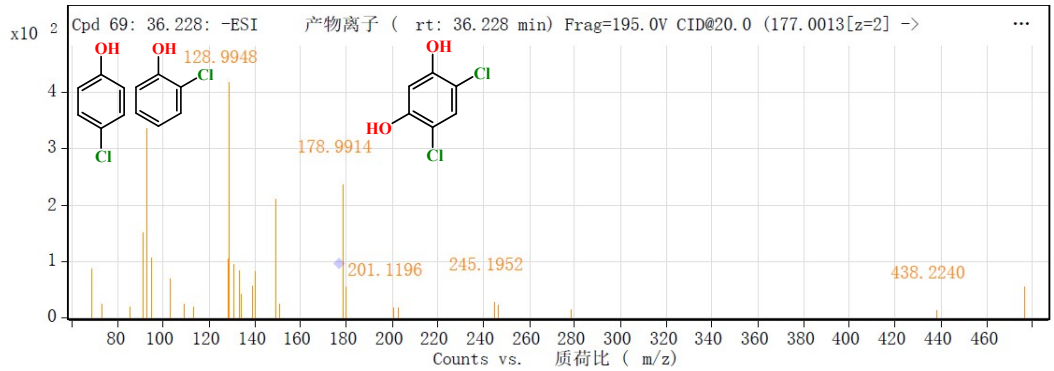

Fig. S25 The intermediates generated during 2,4-DCP degradation on Lac@Tp-TPA.

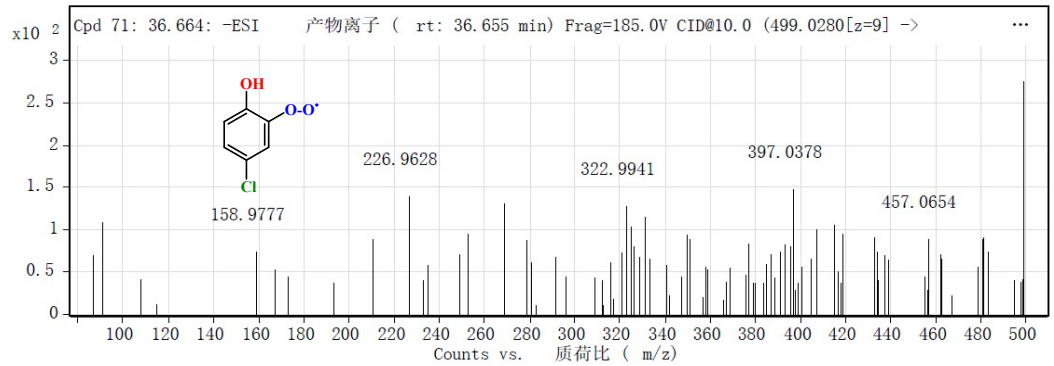

Fig. S26 The intermediates generated during 2,4-DCP degradation on Lac@Tp-TPA.

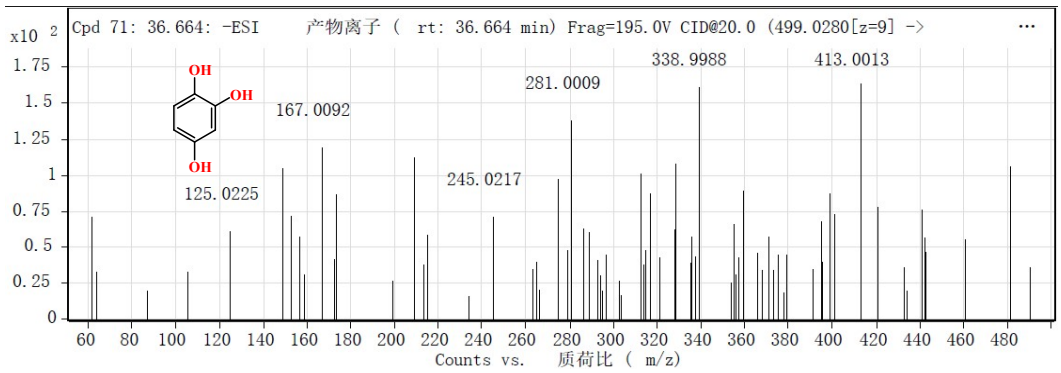

Fig. S27 The intermediates generated during 2,4-DCP degradation on Lac@Tp-TPA.

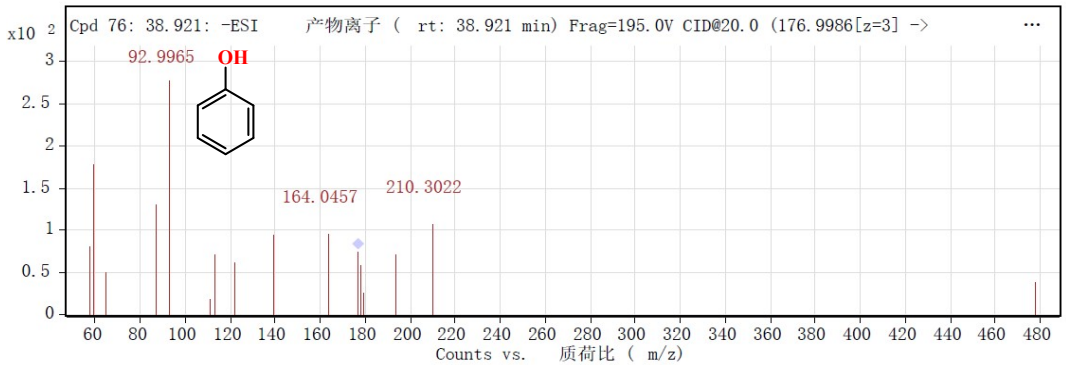

Fig. S28 The intermediates generated during 2,4-DCP degradation on Lac@Tp-TPA.

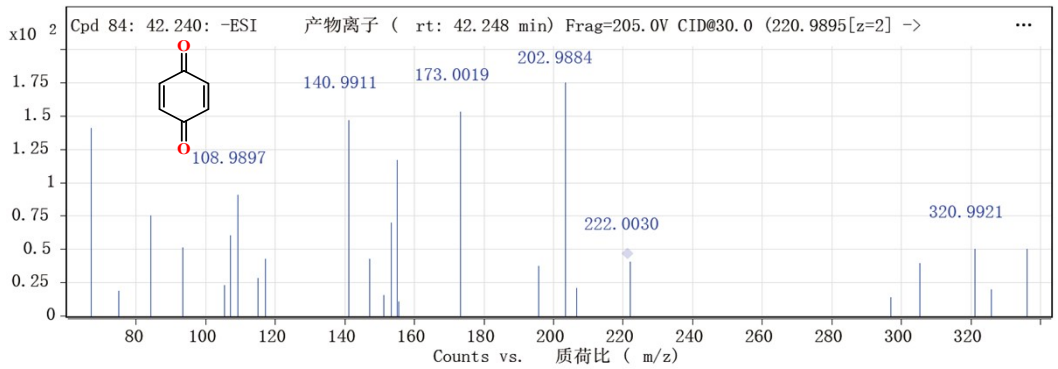

Fig. S29 The intermediates generated during 2,4-DCP degradation on Lac@Tp-TPA.

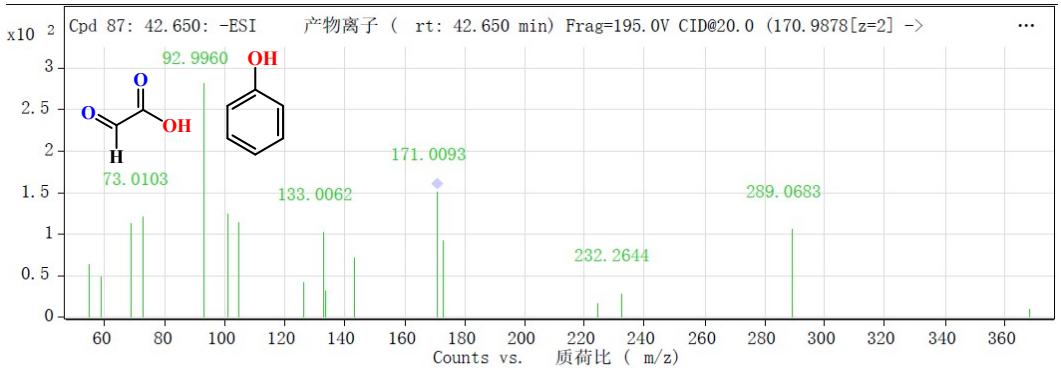

Fig. S30 The intermediates generated during 2,4-DCP degradation on Lac@Tp-TPA.

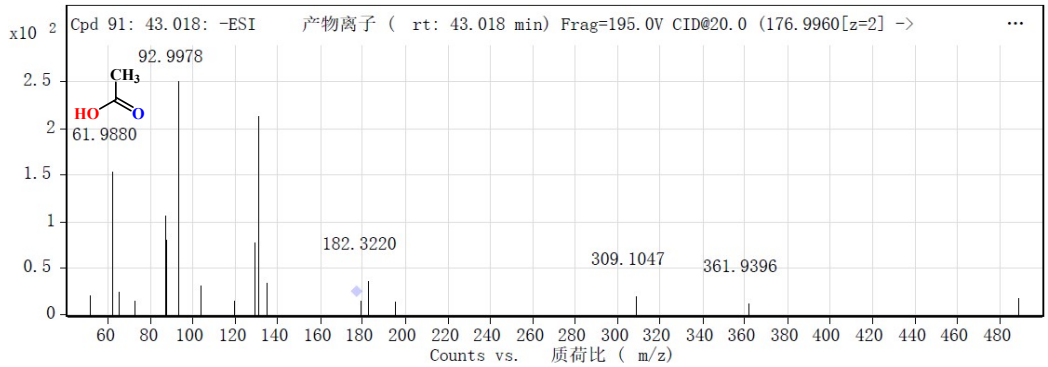

Fig. S31 The intermediates generated during 2,4-DCP degradation on Lac@Tp-TPA.

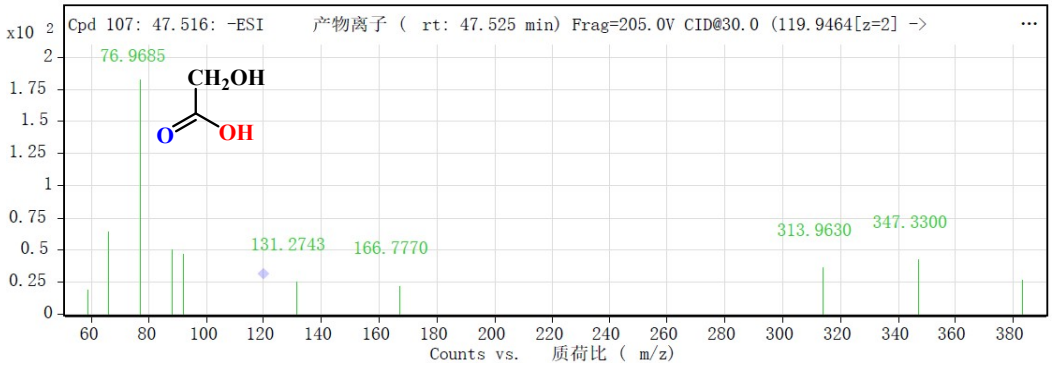

Fig. S32 The intermediates generated during 2,4-DCP degradation on Lac@Tp-TPA.

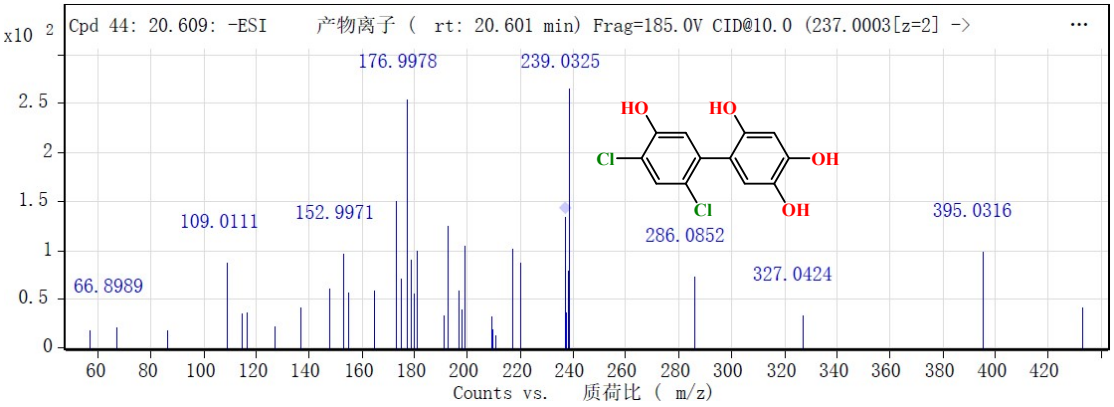

Fig. S33 The intermediates generated during 2,4-DCP degradation on Lac@Tp-TPA.

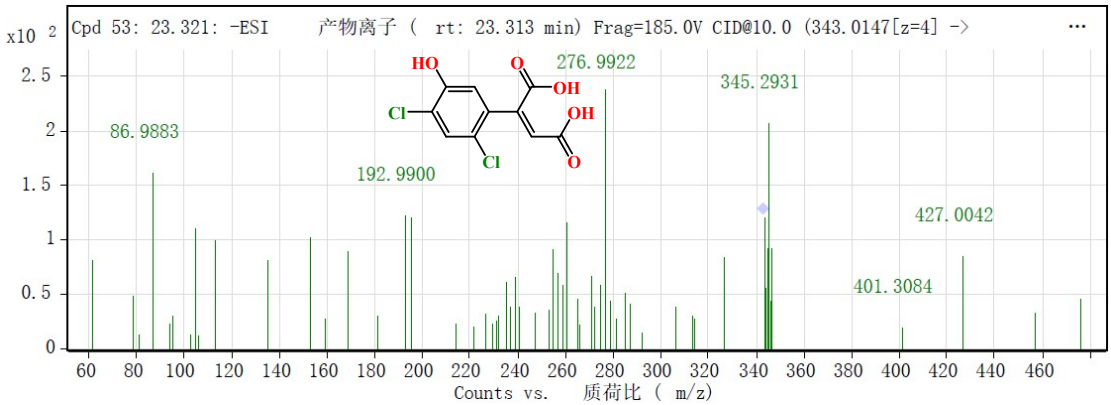

Fig. S34 The intermediates generated during 2,4-DCP degradation on Lac@Tp-TPA.

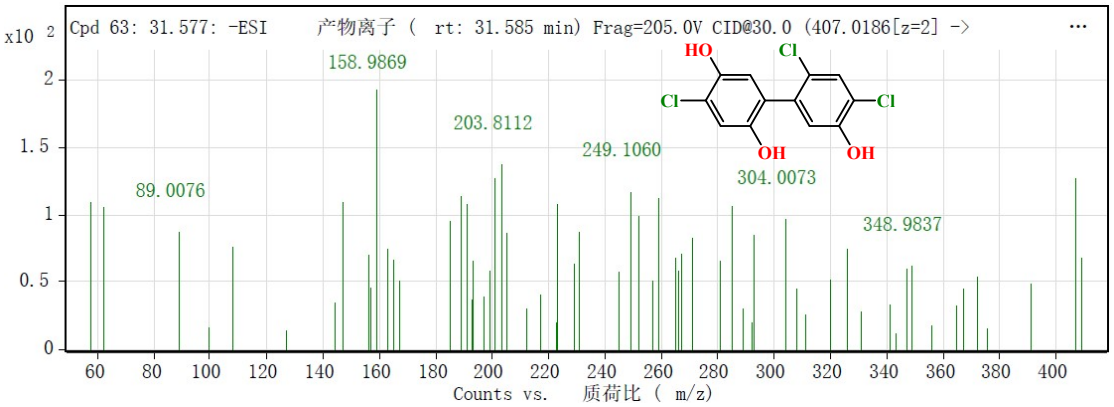

Fig. S35 The intermediates generated during 2,4-DCP degradation on Lac@Tp-TPA.

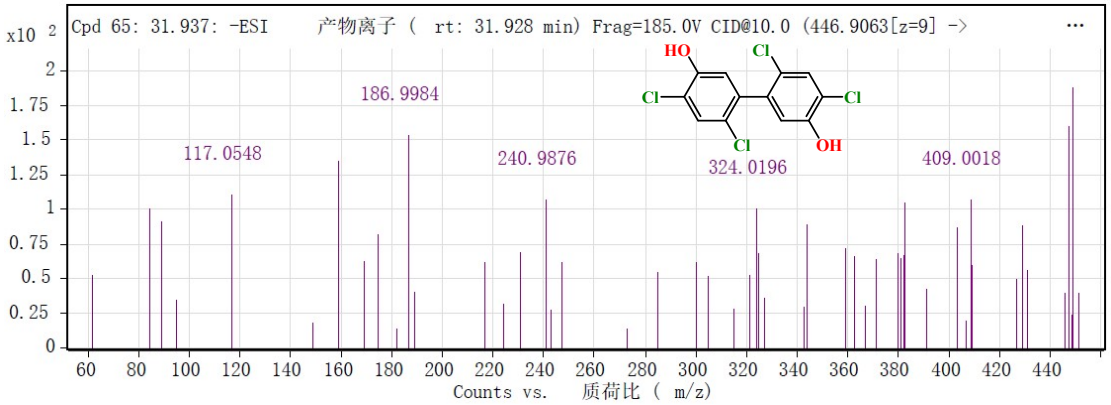

Fig. S36 The intermediates generated during 2,4-DCP degradation on Lac@Tp-TPA.

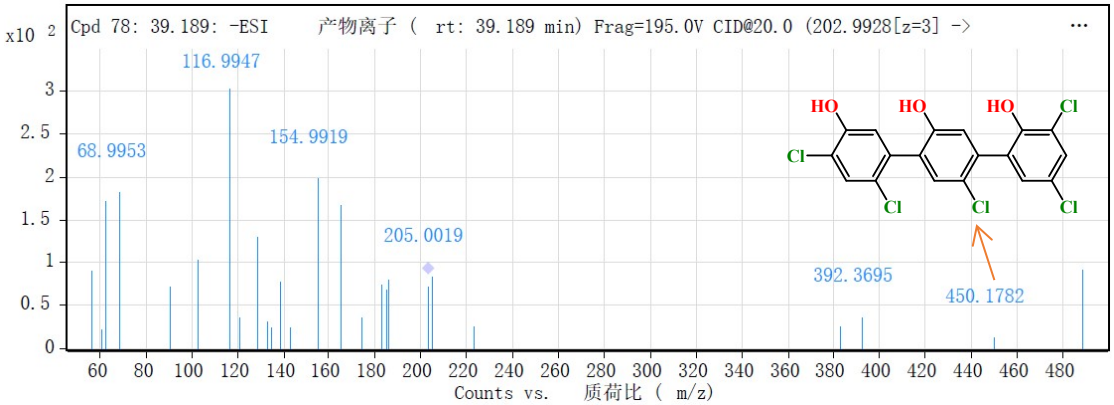

Fig. S36 The intermediates generated during 2,4-DCP degradation on Lac@Tp-TPA.

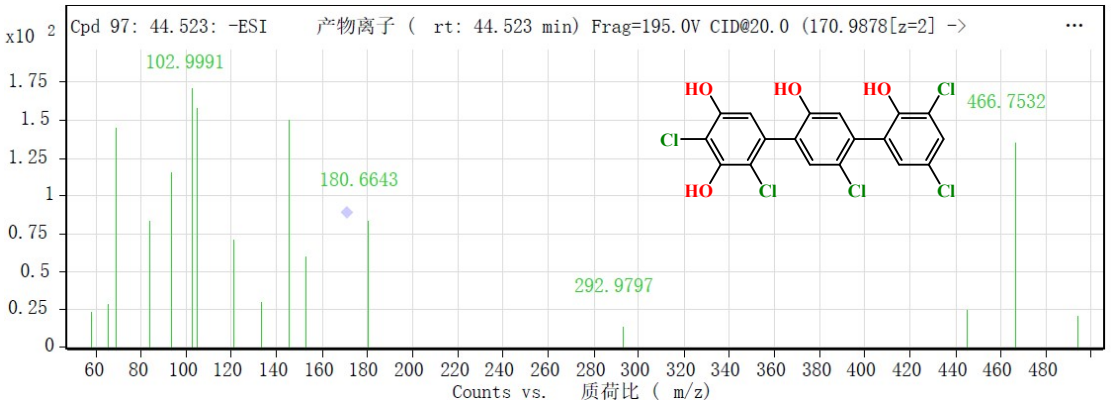

Fig. S37 The intermediates generated during 2,4-DCP degradation on Lac@Tp-TPA.